Journal of Power Sources 222 (2013) 340–343

Contents lists available at SciVerse ScienceDirect

Journal of Power Sources

journal homepage: www.elsevier.com/locate/jpowsour

Short communication

Multi-walled carbon nanotube modified with methylene blue under ultraviolet irradiation as a platinum catalyst support for methanol oxidation

Guotao Yang [a], Xikun Yang [b], Mingli Xu [c,*], Chungang Min [b], Haifeng Xiao [b], Kezhu Jiang [b], Linyan Chen [b], Guanghua Wang [b]

[a] Department of Chemical Engineering, Kunming University of Science and Technology, Kunming 650093, PR China
[b] Research Center for Analysis and Measurement, Kunming University of Science and Technology, Kunming 650093, PR China
[c] Department of Science, Kunming University of Science and Technology, Kunming 650093, PR China

HIGHLIGHTS

- MWCNT is first modified with methylene blue during ultraviolet irradiation.
- Pt nanoparticles are uniformly dispersed on functionalized MWCNT.
- Pt/f_1−MWCNT shows excellent catalytic activity and stability for methanol oxidation.

ARTICLE INFO

Article history:
Received 2 July 2012
Received in revised form
22 August 2012
Accepted 23 August 2012
Available online 10 September 2012

Keywords:
Electrocatalyst
Multi-walled carbon nanotube
Methylene blue
Methanol oxidation
Ultraviolet irradiation

ABSTRACT

To improve the utilization and activity of anodic catalysts for direct methanol fuel cells, multi-walled carbon nanotube (MWCNT) is used as a support for platinum (Pt) nanoparticles synthesized by method of ultraviolet irradiation. MWCNT is modified by methylene blue (f_0-MWCNT) under ultraviolet light (f_1-MWCNT), and then Pt nanoparticles are assembled on the f_1-MWCNT to form composites (Pt/f_1−MWCNT). Fourier transform infrared spectroscopy analysis reveals that the surface of MWCNT is successfully functionalized. Transmission electron microscopy and X-ray diffraction analyses exhibit that the uniformly dispersed Pt nanoparticles of around 2.5 nm in size are obtained. Cyclic voltammetric and chronoamperometric experiments demonstrate that the as-prepared Pt/f_1−MWCNT composites show higher catalytic activity and better stability compared with Pt/f_0−MWCNT and commercial Pt/C (JM), which is vital to anode electrocatalysis in direct methanol fuel cells.

1. Introduction

Direct methanol fuel cells (DMFCs) have attracted much attention for their potential application as clean and mobile power sources with high energy density and simple structure [1–3]. In order to successfully realize the commercialization of DMFCs at low cost, the amount of electrocatalysts should be reduced remarkably while maintaining high mass specific current density. It is very important that metal nanoparticles can be uniformly deposited on support materials. In recent years, Multi-walled carbon nanotube (MWCNT) has attracted considerable interest due to its unique tubular structure, mechanical properties, excellent chemical and thermal stability and, in some cases, even good electrical conductivity as a catalyst support in fuel cells [4,5]. However, the inert surface and the formation of tangled bundles make it difficult to disperse in precursor solutions and colloidal solutions. Several methods, such as oxidative treatment [6–10], polymer wrapping [11–13] and sidewall functionalization [14,15], have been proposed to solve these problems. But the challenge of getting excellent and uniformly dispersed Pt nanoparticles with controllable particle size is still faced with us [16].

In this paper, colloidal Pt nanoparticles were synthesized by method of ultraviolet irradiation. MWCNT modified with methylene blue during ultraviolet irradiation was as a new support of Pt nanoparticles (Pt/f_1−MWCNT). For comparison, Pt nanoparticles were also assembled to MWCNT modified with methylene blue without ultraviolet irradiation (Pt/f_0−MWCNT). The composites were characterized by Fourier transform infrared spectroscopy (FTIR), transmission electron microscopy (TEM) and X-ray diffraction (XRD). The catalytic activity and stability of Pt/f_1−MWCNT for

* Corresponding author. Tel.: +86 0871 5110975; fax: +86 0871 5111617.
E-mail address: xumingli0326@gmail.com (M. Xu).

0378-7753/$ – see front matter © 2012 Elsevier B.V. All rights reserved.
http://dx.doi.org/10.1016/j.jpowsour.2012.08.074

methanol oxidation in alkaline solution were investigated in comparison with Pt/f_0–MWCNT and commercial Pt/C (20 wt.% Pt).

2. Experimental

2.1. Functionalization of MWCNT

The functional process of MWCNT was as follows: 100 mg MWCNT (Shenzhen Nanotech Port Co. Ltd., Shenzhen, China) and 10 mg methylene blue (MB) were respectively weighed out into a quartz tapered bottle, and then 50 mL of double distilled water was added. After that, the mixture was magnetically stirred under ultraviolet (UV) light with the wavelength of 254 nm at room temperature for 6 h. Next, the mixture was centrifuged, filtered and washed with plenty of double distilled water for the sake of thoroughly removing the excess MB. Ultimately, the filter cake was vacuum dried overnight at 333 K. The obtained product was marked as f_1-MWCNT. For comparison, the same content mixture was only magnetically stirred without UV irradiation. After the same procedure, the corresponding product was labeled as f_0-MWCNT.

2.2. Preparation of nanocatalysts

Pt nanoparticles were synthesized by method of ultraviolet irradiation. Briefly, H_2PtCl_6 (3.08 mM) was mixed with acetone (0.108 M) as well as polyethylene glycol (PEG-400, 0.09 M) in a quartz tapered bottle, and then the precursor solution was exposed to ultraviolet irradiation until the recorded curves of ultraviolet–visible (UV–Vis) spectra did not change. Pt colloidal solution was obtained.

Pt/f_1–MWCNT composites (20 wt.% Pt) were prepared as follows: 192 mg f_1-MWCNT was added into 100 mL of the previously prepared Pt colloidal solution. The mixture was stirred vigorously for 3 h at room temperature. The resulting solids were filtered, washed with copious double distilled water, and vacuum dried overnight at 333 K to obtain Pt/f_1–MWCNT nanocatalysts. By comparison, Pt/f_0–MWCNT nanocatalysts with 20 wt.% Pt were synthesized according to the same procedure.

2.3. Measurement

FTIR measurements were carried out on an FTS-40 Fourier transform infrared spectrometer at a resolution of 4 cm^{-1}. UV–Vis spectra were recorded on a lambda 900 UV/Vis/NIR spectrophotometer. XRD data were obtained by mean of using a Bruker D8 Advance X-ray diffractometer with Cu Kα (0.15,406 nm) radiation. TEM images were taken on a JEOL JEM-2100 electron microscope (200 kV).

All electrochemical measurements were carried out on a CHI760C electrochemistry work station at 303 K. A typical suspension of the nanocatalyst ink was prepared by dispersing 2 mg of the nanocatalyst powder in 1 mL solution with 1:19 volume ratio of nafion (5%) and isopropanol. Then 10 μL of this ink was pipetted onto a polished glass carbon (GC) electrode and dried in air at room temperature. A traditional three-electrode cell was used with a platinum wire as the counter electrode, a saturated calomel electrode (SCE) as the reference electrode and the previously prepared GC electrode as the working electrode. Cyclic voltammetric and chronoamperometric experiments were conducted in 0.5 M KOH + 2 M methanol aqueous solution. Prior to testing, the electrolyte solution (0.5 M KOH) was deaerated by bubbling pure nitrogen for 20 min.

3. Results and discussion

3.1. FTIR analysis

FTIR spectra of pristine MWCNT, f_0-MWCNT and f_1-MWCNT are shown in Fig. 1. It can be seen from Fig. 1a that the peak at 1580 cm^{-1} attributed to the C=C stretching vibrations is the characteristic peak of MWCNT. As shown in Fig. 1b, the peaks at 1570 cm^{-1} and 1650 cm^{-1} are probably ascribed to the C=C stretching vibrations of MWCNT and MB, respectively. This indicates that MB has been physically or chemically adsorbed by MWCNT. But C=C characteristic peak of MWCNT is shifted, presumably implying the appearance of interaction between MWCNT and MB [17–19]. It should be noted from Fig. 1c that the spectrum of f_1-MWCNT is almost similar to that of f_0-MWCNT from 4000 cm^{-1} to 1330 cm^{-1}. The peaks at 1093 cm^{-1} and 667 cm^{-1} may be assigned to C–N stretching vibrations and N–H out-of-plane bending vibrations, respectively. This suggests that reactive and anchoring sites have formed on the surface of MWCNT during UV irradiation.

3.2. UV–Vis analysis

Fig. 2 exhibits UV–Vis absorption spectra of the Pt precursor solution after ultraviolet irradiation. It can be found that the absorbance significantly increases with successive ultraviolet irradiation, but the curves are almost overlapped after 30 min, which suggests that the reaction had been conducted completely and that the colloidal Pt had been generated. As seen in Fig. 2, no plasmon absorbance could be detected between 300 and 700 nm for Pt nanoparticles and the consequence is in accordance with the results reported by Masafumi Harada et al. [20].

3.3. TEM and XRD analyses

Fig. 3a–c shows the typical TEM images of the synthesized Pt/f_0–MWCNT, Pt/f_1–MWCNT and colloidal Pt nanoparticles. It can be seen from Fig. 3a that the spherical Pt nanoparticles are successfully dispersed on the walls of MWCNT. Although Pt nanoparticles aggregate to form clusters, no free Pt nanoparticles detached from MWCNT can be observed in the TEM image. Fig. 3b exhibits that even though Pt clusters are still found in part of the surface, the dispersion of Pt nanoparticles in Pt/f_1–MWCNT

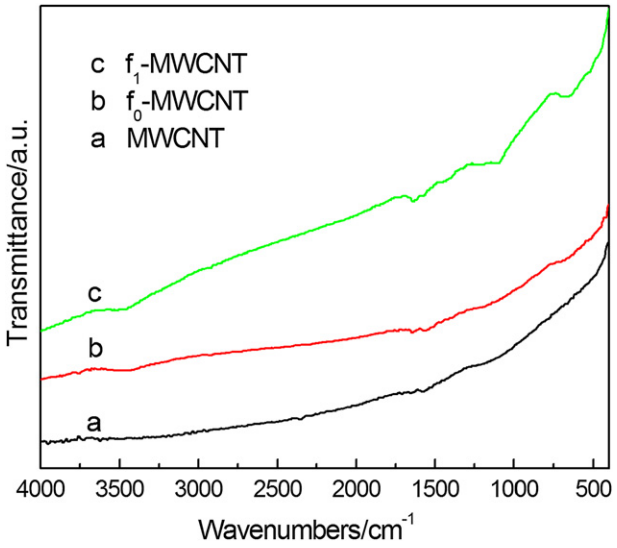

Fig. 1. FTIR spectra of (a) pristine MWCNT, (b) f_0-MWCNT and (c) f_1-MWCNT.

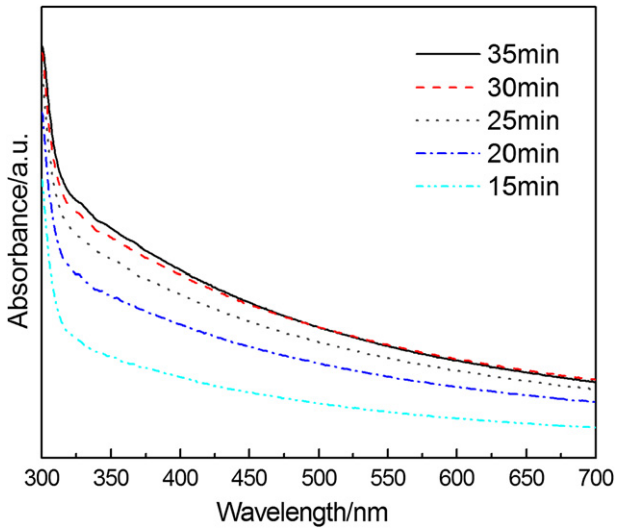

Fig. 2. UV-vis absorption spectra of Pt precursor solution after ultraviolet irradiation.

composites is significantly improved. This can possibly be ascribed to the effect of C–N and N–H groups. In other words, f_1-MWCNT is in favor of the dispersion state of Pt nanoparticles compared with f_0-MWCNT. Fig. 3c shows that crystalline Pt nanoparticles with the mean diameter size of 2.5 nm is successfully prepared by method of ultraviolet irradiation, which can be further confirmed in the following XRD results.

The XRD pattern of Pt/f_1–MWCNT composites is shown in Fig. 3d. The diffraction peaks at ca. 40°, 46°, 68° and 81° are attributed to the (111), (200), (220) and (311) planes of the face-centered cubic structure of Pt crystals, respectively. However, the peak at around 26° is ascribed to the crystalline nature of the graphitic structure of MWCNT. The average particle size of Pt crystals calculated from the Pt (111) plane by using the Debye–Scherrer equation is around 2.7 nm, in good agreement with the value obtained by TEM analysis.

3.4. Electrochemical characterization

The electrochemical properties of Pt/f_1–MWCNT, compared with Pt/f_0–MWCNT and the commercial Pt/C, have been investigated by method of the cyclic voltammetry at a potential scan rate of 50 mV s^{-1} in 0.5 M KOH + 2.0 M CH_3OH aqueous solution, and the stabilized cyclic voltammertric curves are depicted in Fig. 4a. It is clear from Fig. 4a that the mass specific current density of Pt/f_1–MWCNT is higher than that of Pt/f_0–MWCNT and the commercial Pt/C catalyst. The peak current densities due to methanol oxidation in the forward sweep for Pt/f_1–MWCNT, Pt/f_0–MWCNT and Pt/C are 2035 mA mg^{-1} Pt, 1246 mA mg^{-1} Pt and 959 mA mg^{-1} Pt, respectively. The Pt/f_1–MWCNT catalyst exhibits a mass specific current density 1.63 times higher than the Pt/f_0–MWCNT catalyst and 2.12 times higher than the Pt/C catalyst. Therefore, the Pt/f_1–MWCNT catalyst is much more active for methanol oxidation. Furthermore, the onset potential of Pt/f_1–MWCNT is almost comparable with that of the commercial Pt/C catalyst, while the onset potential of Pt/f_0–MWCNT is lower than that of the commercial Pt/C catalyst. Higher current density and lower onset potential are two significant factors to assess the performance of electrocatalysts. The higher peak current density and lower onset potential for methanol oxidation imply that the Pt/f_1–MWCNT catalyst has excellent catalytic activity.

Fig. 4b describes the chronoamperometric curves of Pt/f_1–MWCNT, Pt/f_0–MWCNT and the Pt/C catalyst at −0.14 V in 0.5 M KOH + 2.0 M CH_3OH aqueous solution. For all the catalysts, the current density decrease with time, probably because of the catalyst poisoning by adsorbed CO species resulting from methanol oxidation and the consumption of hydroxide ions which are responsible for the oxidation of CO species [21,22]. However, the Pt/f_1–MWCNT catalyst is able to maintain the highest current density

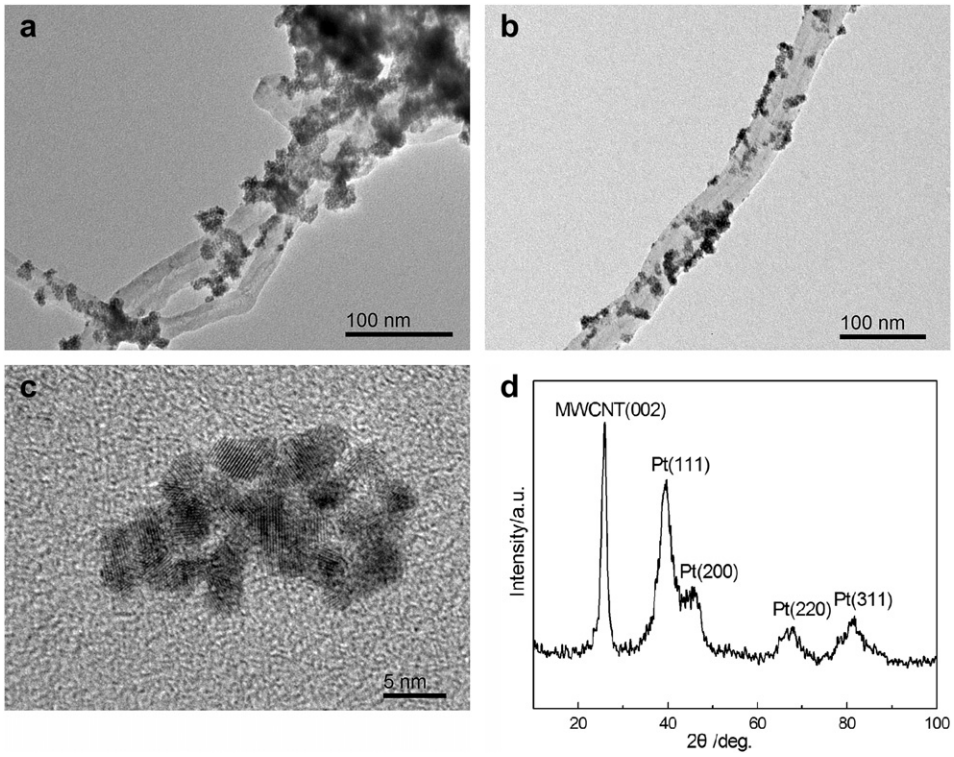

Fig. 3. TEM images of (a) Pt/f_0-MWCNT and (b) Pt/f_1-MWCNT composites. (c) HRTEM image of colloidal Pt nanoparticles. (d) XRD pattern of Pt/f_1-MWCNT composites.

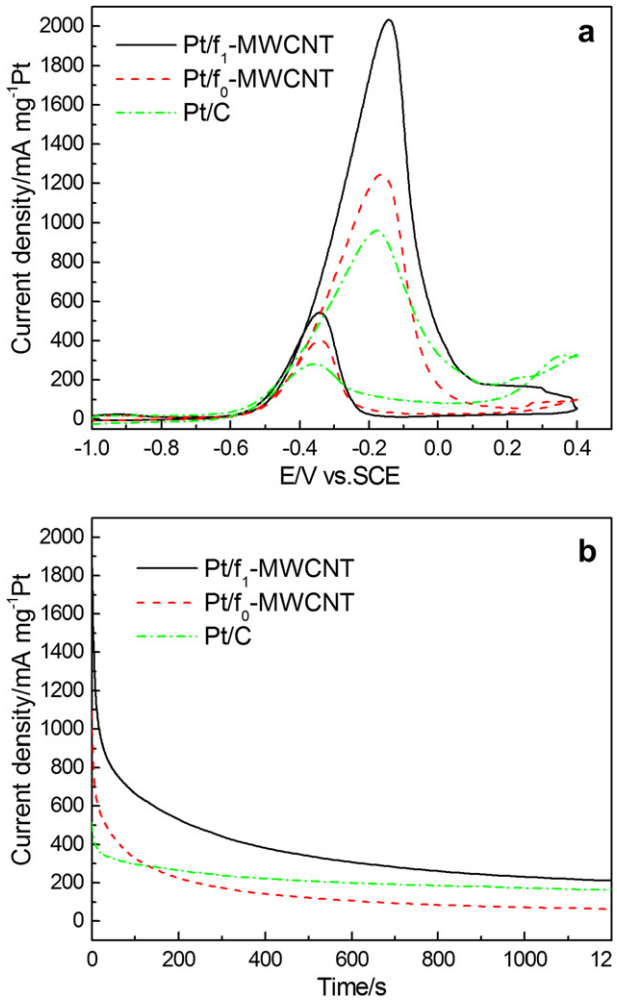

Fig. 4. (a) Cyclic voltammograms of various electrodes at 50 mV s^{-1} in 0.5 M KOH + 2.0 M CH_3OH aqueous solution. (b) Chronoamperograms of various electrodes at −0.14 V in 0.5 M KOH + 2.0 M CH_3OH aqueous solution.

in the whole process. This indicates that the Pt/f_1−MWCNT catalyst exhibits higher catalytic activity and better stability than both Pt/f_0−MWCNT and Pt/C.

4. Conclusions

The comparative study of MWCNT modified by MB, with and without ultraviolet irradiation, revealed that MWCNT modified with MB under ultraviolet irradiation was in favor of the dispersion state of Pt nanoparticles and could enhance the catalytic performance of Pt nanoparticles. FTIR analysis showed that the C−N and N−H groups existed on the surface of MWCNT to provide reactive and anchoring sites. TEM and XRD exhibited that the dispersion of Pt nanoparticles of around 2.5 nm in size was relatively homogeneous on f_1-MWCNT. Electrochemical studies using cyclic voltammetry and chronoamperometry indicated that the Pt/f_1−MWCNT catalyst exhibited higher catalytic activity and better stability than the Pt/f_0−MWCNT catalyst and the commercial Pt/C catalyst. All these results demonstrate that the synthesized Pt/f_1−MWCNT catalyst is a promising anode catalyst for DMFCs.

Acknowledgments

This work was financially supported by the National Natural Science Foundation of China (Nos. 51164017, 20863003).

References

[1] B.D. Lee, D.H. Jung, Y.H. Ko, J. Power Sources 131 (2004) 207–212.
[2] R. Dillon, S. Srinivasan, A.S. Aricò, V. Antonucci, J. Power Sources 127 (2004) 112–126.
[3] T. Zhang, Q.M. Wang, J. Power Sources 140 (2005) 72–80.
[4] J.J. Gooding, Electrochim. Acta 50 (2005) 3049–3060.
[5] S.N. Marinković, J. Serb, Chem. Soc. 73 (2008) 891–913.
[6] X.L. Chen, W.S. Li, C.L. Tan, Y.Z. Wu, J. Power Sources 184 (2008) 668–674.
[7] C.E. Banks, A. Crossley, C. Salter, S.J. Wilkins, R.G. Compton, Angew. Chem. 45 (2006) 2595–2599.
[8] X. Zhong, X. Zhang, X. Sun, B. Liu, Y. Kuang, J. Chen, Chin. J. Chem. 27 (2009) 56–62.
[9] C. Yang, X. Hu, D. Wang, C. Dai, L. Zhang, H. Jin, S. Agathopoulos, J. Power Sources 160 (2006) 187–193.
[10] Z.C. Wang, D.D. Zhao, G.Y. Zhao, H.L. Li, J. Solid State Electrochem 13 (2009) 371–376.
[11] S. Wang, F. Yang, S.P. Jiang, S. Chen, X. Wang, Electrochem. Commun. 12 (2010) 1646–1649.
[12] S.K. Cui, D.J. Guo, J. Colloid Interface Sci. 333 (2009) 300–303.
[13] S.F. Zheng, J.S. Hu, L.S. Zhong, L.J. Wan, W.G. Song, J. Phys. Chem. C 111 (2007) 11174–11179.
[14] M.S. Saha, R. Li, X.L. Sun, J. Power Sources 177 (2008) 314–322.
[15] G.D. Vuković, M.D. Obradović, A.D. Marinković, J.R. Rogan, P.S. Uskoković, V.R. Radmilović, S.L. Gojkovi&cacute, Mater. Chem. Phys. 130 (2011) 657–664.
[16] K. Lee, J.J. Zhang, H.J. Wang, D.P. Wilkinson, J. Appl. Electrochem. 36 (2006) 507–522.
[17] L.H. Ai, C.Y. Zhang, F. Liao, Y. Wang, M. Li, L.Y. Meng, J. Jiang, J. Hazard. Mater. 198 (2011) 282–290.
[18] B.G. Cousins, A.K. Das, R. Sharma, Y. Li, J.P. McNamara, L.H. Hillier, L.A. Kinloch, R.V. Ulijn, Small 5 (2009) 587–590.
[19] M. Kojima, T. Chiba, J. Niishima, T. Higashi, T. Fukuda, Y. Nakajima, S. Kurosu, T. Hanajiri, K. Lshii, T. Maekawa, A. Inoude, Nanoscale Res. Lett. 6 (2011) 128–133.
[20] M. Harada, K. Saijo, N. Sakamoto, Colloids Surf. A 349 (2009) 176–188.
[21] M.A. Scibioh, S.K. Kim, E.A. Cho, T.H. Lim, S.A. Hong, H.Y. Ha, Appl. Catal. B 84 (2008) 773–782.
[22] F.H.B. Lima, E.R. Gonzalez, Appl. Catal. B 79 (2008) 341–346.